



LAWRENCE
LIVERMORE
NATIONAL
LABORATORY

LLNL-JRNL-679035

The effect of temperature and microstructure on dynamic deformation of iron, tantalum, and titanium

L. E. Chen, D. C. Swift, J. N. Florando, J. Hawreliak, A. Lazicki, R. A. Austin, M. D. Saculla, D. Eakins, J. V. Bernier, M. Kumar

November 6, 2015

Journal of Applied Physics

Disclaimer

This document was prepared as an account of work sponsored by an agency of the United States government. Neither the United States government nor Lawrence Livermore National Security, LLC, nor any of their employees makes any warranty, expressed or implied, or assumes any legal liability or responsibility for the accuracy, completeness, or usefulness of any information, apparatus, product, or process disclosed, or represents that its use would not infringe privately owned rights. Reference herein to any specific commercial product, process, or service by trade name, trademark, manufacturer, or otherwise does not necessarily constitute or imply its endorsement, recommendation, or favoring by the United States government or Lawrence Livermore National Security, LLC. The views and opinions of authors expressed herein do not necessarily state or reflect those of the United States government or Lawrence Livermore National Security, LLC, and shall not be used for advertising or product endorsement purposes.

The effect of temperature and microstructure on dynamic deformation of iron, tantalum, and titanium

L. E. Chen,^{1,a)} D. C. Swift,² J. N. Florando,² J. Hawrelak,² A. Lazicki,² R. A. Austin,² M. D. Saculla,² D. Eakins,¹ J. V. Bernier,² and M. Kumar²

¹⁾*Institute of Shock Physics, Imperial College London, SW7 2BW UK*

²⁾*Lawrence Livermore National Laboratory, Livermore, CA 94550 USA*

(Dated: 10 August 2015)

Laser-driven shock loading was performed on thin samples of iron, tantalum, and titanium at strain-rates up to 10^7 s $^{-1}$, and over a range of temperatures extending from 120 through 800 K, to investigate the influence of temperature on the early stages of yielding and plastic flow in materials of distinct crystal structure and initial defect density. The onset of yielding was identified using time-resolved velocimetry of the target rear surface to reveal the peak elastic state in the precursor wave front. Measurements on as-received iron reveal a trend of decreasing peak elastic stress (σ_E) with increasing temperature and electron microscopy of the recovered material revealed evidence of mobile dislocations coalescing into subgrains. This is in contrast to the results for the annealed iron where the σ_E remains constant with increasing temperature and recovered samples showed indications of deformation twinning. For tantalum, the yield strength remains constant for the most part, but has a jump in yield strength at 815 K, indicative of a possible twinning to slip transition with increasing temperature. For titanium, the yield strength was generally constant with temperature. These results provide insight into studying deformation mechanisms, such as slip and twinning, in high rate loading of materials.

I. INTRODUCTION

Studying the effect of temperature and microstructure on dynamic strength of materials is important for applications ranging from condensed matter physics studies to nuclear engineering. Under dynamic loading, a shock will be generated in a material and as it propagates through, the faster moving elastic compression wave separates from the plastic wave. Deformation sources, such as dislocations or twins, in the plastic wave emit elastic relaxation wavelets through the compressed material ahead which contribute to the sharp decay in elastic shock amplitude during the initial stages of deformation^{1–3} which allows the material to reach an equilibrium elastic limit. For this reason, the relaxation behavior of the elastic wave is innately tied to the plastic deformation behind it. This paper aims to describe plastic deformation mechanisms as a function of temperature and microstructure to understand material strength and relaxation.

It has been seen in several materials that flow stress as well as the peak elastic stress of a material increases as the strain rate increases^{4–9}. Temperature dependence has also been investigated for bcc, hcp, and fcc materials. Generally, under quasi-static and low strain rate loading conditions, the yield strength of bcc metals will decrease with increasing temperature as a result of thermal fluctuations contributing to the thermal activation required for dislocation propagation. Due to the close-packed geometric configuration of the dislocation core¹⁰, fcc metals have a significantly lower Peierls' stress than bcc. Therefore, bcc metals have a more noticeable dependence on thermal assistance to overcome Peierls' barriers,

as fcc metals have an over-sensitivity and will have a less pronounced thermal dependence. Rather, for fcc metals, motion is limited by the athermal process of dislocation breakaway from dislocation forests^{11,12}. Hcp metals are considered to have behavior somewhere between bcc and fcc metals^{12,13}. In particular, hcp titanium has a Peierls' stress closer to that of bcc¹⁰.

At higher strain rates, it has been seen for some materials with strong nonlinear properties, including aluminium and copper, that the peak elastic stress will appear increase as a function of increasing temperature as a result of dislocation drag effects^{14–18}. Additionally, as mentioned before, there is a possibility for several materials that under certain conditions, deformation will occur by twinning^{12,13,19,20}, which can be said to present a more modest, nearly athermal, temperature dependence^{6,19,21–24}. Previous work on bcc metals at high strain rates showed that at a range of strain rates, temperature-dependent yield behavior of bcc metals would vary depending on whether conditions favored twinning or slip^{19,25–27}.

Factors that dictate whether a material will twin or slip include inherent material properties along with external loading conditions. Fcc and hcp metals with low stacking fault energies, like copper^{28–30} have a higher propensity to twin even under quasi-static loading at ambient conditions. Some bcc metals have shown signs of twinning at either low temperatures or high strain rate loading^{19,31–35}. Additionally, Arnold saw a strong dependence of twinning as a function of grain size in dynamic loading experiments^{20,36}. Thus, in addition to inherent material susceptibility, twinning is favored over slip at low temperatures, high strain rates, large grain sizes, and high strains.

There has been a great deal of effort into studying

^{a)}Electronic mail: l.chen11@imperial.ac.uk

the nucleation and growth of twins. For fcc metals, it had originally been proposed by Cottrell and Bilby and developed by several other researchers that a type of pole mechanism was responsible for twin nucleation and growth³⁷⁻⁴⁴. However, this mechanism would not be possible for bcc or hcp metals as the energetics and geometry cannot satisfactorily describe what is found empirically^{42,43,45} and the circumstantial evidence for the mechanisms governing twinning fcc metals was inconsistent with what was found in recovered samples⁴⁶⁻⁴⁸. Thus other mechanisms have been put forth^{43,45-47,49-51}. Particular focus in this paper will be put on mechanisms for bcc metals, specifically in regards to the mechanisms proposed by Mahajan and by Lagerlof. Both the mechanisms describe a similar process for twin nucleation, and differ in describing twin growth. Mahajan describes twin growth as the coalescence of nucleated twins in opportunistic encounters via a “slip band conversion” model. Lagerlof describes twin growth through a “double cross-slip” model based off of mechanism first proposed by Pirouz for describing twinning in silicon^{45,52}. For the purposes of this paper, it is of interest to understand the potential mechanisms for twin nucleation, as that will lend insight into the slip/twinning transition in materials.

For bcc, both models by Mahajan and Lagerlof agree and it is now widely accepted that nucleation depends on dissociation of a screw dislocation into 3 partials as

$$\frac{a}{2} \langle 111 \rangle \rightarrow 3 \times \frac{a}{6} \langle 111 \rangle \quad (1)$$

on adjacent $\{112\}$ planes^{45,48-50}. From here, the partials may coalesce, resulting in slip, or they may dissociate further, with a leading partial expanding to produce a loop faster than a trailing (or sessile) partial, resulting in a faulted region. Thus, twin nucleation is dependent on factors favoring dissociation over coalescence of the constituting partials.

Forces influencing dissociation are dislocation line tension, stacking fault energy (SFE), lattice resistance (Peierls' stress), and interaction force between partials^{45,53}. The dependency on these forces drives the conditions which are known to favor twinning deformation, namely low temperatures, high stresses, increased strains, and larger grain sizes. As slip mechanisms will not have to overcome additional forces of SFE and interaction force, it imposes the need for high stresses for twinning to occur. Following that, large grains and large strains allow for longer dislocation lengths. As with Frank Read sources, a longer dislocation will have a lower magnitude line tension and will therefore require less stress to bow out. Line tension is given by

$$\tau_{LT} = \frac{\alpha \mu b}{L/2} \quad (2)$$

where α is a constant, μ is a lattice resistance term related to Peierls stress, b is Burgers vector, and L is dislocation length⁴⁵. In addition to grain size dependence,

there is a strong temperature dependence for the onset of twinning. As stated before, for twinning to occur, there needs to be a glissile leading partial and a sessile trailing partial, or else the partials will coalesce and slip will occur. The conditions for activation of either partial depends on its respective Burgers vector as well as lattice resistance, which is dependent on temperature. At low temperatures it is possible to have one partial, the leading partial, move faster than another partial, the trailing partial, which may move slowly or even not at all. As leading partial grows, it increases in length, which in turn allows it to increase its velocity (due to lower line tension), resulting in an feedback process known as “explosive dissociation”⁵³.

This work compares bcc metals iron and tantalum and hcp metal titanium under similar loading conditions to further understand what role microstructure plays in the onset of plastic flow and how that process influences temperature dependence. There is much to be understood regarding the complex interplay of material deformation mechanisms at high strain rates, accounting for thermal activation, twinning, dislocation generation vs mobility, and nonlinear elastic properties which governs continuum-level properties such as strength. By evaluating these factors, models can be made to better predict the constitutive response of materials under high-rate deformation.

II. EXPERIMENTAL METHODS

High strain-rate pressure waves were applied to the iron, tantalum, and titanium samples using the high powered laser-system at Trident Laser Facility at Los Alamos National Laboratory. The drive beam operated at 527 nm. For the annealed iron, tantalum, and titanium drive energies were approximately 200 J on a 5 mm spot. For the as-received iron, a 1 mm spot size was focused on the target and the drive energy was approximately 60 J. The loading conditions were changed once it was discovered that in some metals, the 1 mm spot required significantly lower energy input to attain the desired irradiance which was more difficult to control and often the spot was too focused and would ablate through the foil, making it more difficult to produce a stable wave profile. The pulse shapes were constructed for the iron such that the rise times of several hundred picoseconds. Pulse lengths were all 5 ns in length and had gradual increase in energy of 30% of the total energy to sustain a constant pressure during the pulse. For these experiments, the primary diagnostic was a pair of line-imaging VISARs which interferometrically measured the particle velocity at the rear surface of the target. The VISARs used different etalons to vary the time delay in each interferometer. One of the VISARs had smaller etalon with velocity-per-fringe (VPF) of 1.50 km/s per fringe to give greater time sensitivity with a time delay of 140 ps for determining strain rate and a higher VPF to confirm peak

stress state, while the other had smaller VPF of 0.498 km/s per fringe for better velocity sensitivity to accurately reveal the yield amplitude, with a time delay of 200 ps.

The annealed and as-received iron came in 125 and 100 micron foils, respectively, and were purchased from Goodfellow, Cambridge Limited. The thinner as-received iron meant that we would be probing the material while it was at higher strain rate compression, but for the purposes of this analysis, the magnitudes of the peak elastic stresses were not directly compared between the two materials, rather the temperature dependent behavior and the deformation mechanisms investigated via recovery. Therefore, it was not necessary to incorporate the strain rate differences into the VISAR analysis. The purity of the annealed and as-received iron was 99.99% and 99.5%, respectively. Tantalum was 99.9% purity, 100 microns. Titanium was 99.6% purity and 125 microns thick. Microscopy indicated the as-received iron had a dislocation density of 1×10^9 per m² and the annealed iron had a dislocation density of 5×10^8 per m², or approximately half that of the as-received. The dislocation density of the tantalum before loading was found to be 1×10^9 per m². The annealed iron had a rather uniform pattern of grain sizes around 40-50 microns whereas the as-received iron had erratic arrangements of grain structures ranging from 5-20 microns. Tantalum had elongated grains 10-40 microns in diameter. Titanium had grains approximately 20-30 microns.

The targets were 12 mm in diameter and were pressed between two copper washers. The copper washers were pressed in place in the target holder by a set screw.

The target holder was designed to pre-cool targets to temperatures as low as 80 K and pre-heat as high as 800 K. Cooling was accomplished by flowing liquid nitrogen through steel tubing connected to the target holder. The target was held in place by copper washers which made contact with the tubing to ensure maximum conductivity. Two cartridge heaters that were each 3 mm in diameter were inserted into the aluminium body of the target holder on opposite sides of the target and would resistively heat according to an applied voltage up to 40 V. Figure 1 shows a CAD diagram of the target holder. A thermocouple was placed between the copper washer and a copper fixture that was used to hold the tubing in place on the target holder. The thermocouple was used to determine the temperature of the target during the shot and it was paired with a temperature controller to command the voltage supply to the heater cartridges. The accuracy of the temperature is calculated to be within ± 5 K.

There was concern that the heating set-up would anneal the metals. To determine if the samples had been annealed in the target holder, samples of each metal were heated to 800 K for 10 min and hardness measurements were taken. The hardness measurements remained the same after heating, indicating material was not annealed during the experimental set-up.

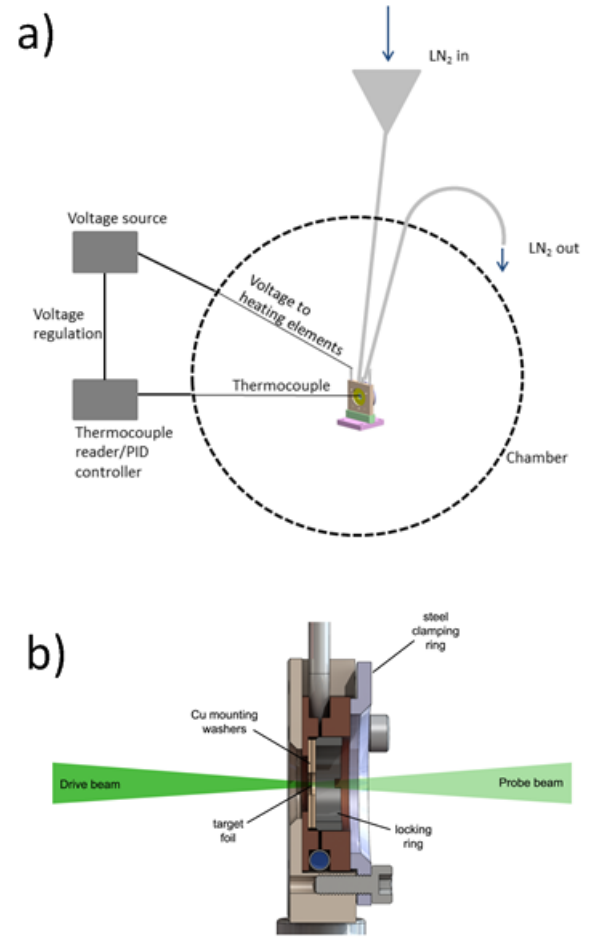


FIG. 1. Target holder used to cool and heat targets from 120 K through 800 K.

III. RESULTS

For all materials, the stress associated with the peak of the elastic wave, σ_E , was calculated. σ_E was obtained by using the Hugonio jump equations to find that

$$\sigma_E = 1/2 \rho u_p c_L \quad (3)$$

where σ_E is peak elastic stress, ρ is initial density u_p is the particle velocity at the peak of the elastic shock, and c_L is the longitudinal wave speed. It is assumed that the sample is not overdriven and the elastic wave is approximately isentropic.

Both the as-received and annealed iron were dynamically loaded under similar loading conditions to strain rates around upper 10^6 s⁻¹. Figure 4 shows the σ_E as a function of temperature. The as-received iron appears to exhibit a trend of decreasing σ_E with increasing temperature, whereas the σ_E of the annealed iron remains relatively constant over the temperature range.

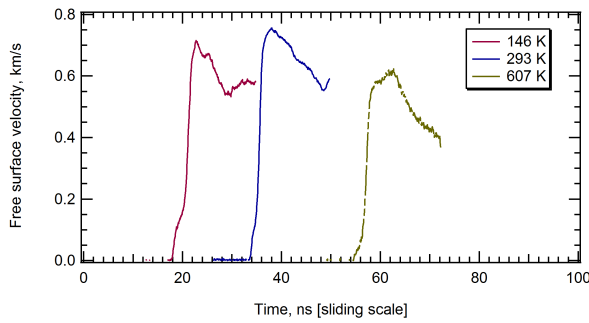


FIG. 2. As-received iron velocimetry as a function of temperature.

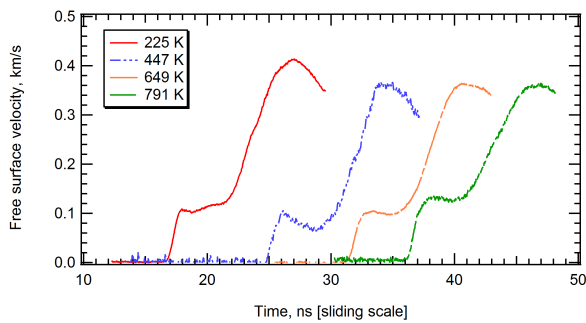


FIG. 3. Annealed iron velocimetry as a function of temperature.

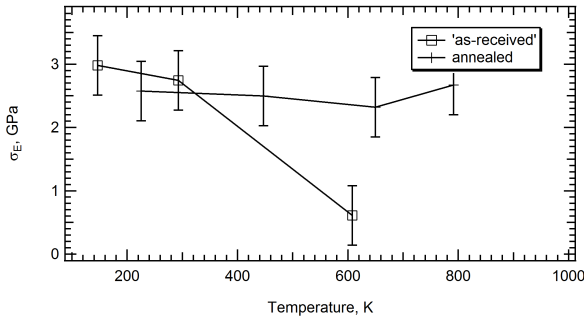


FIG. 4. Annealed and as-received iron σ_E as a function of temperature. The as-received iron shows a trend of decreasing σ_E as temperature increases, whereas the annealed iron demonstrates a nearly athermal response.

TEM of the annealed iron revealed twins, an example of which can be seen in Figure 5. The as-received iron showed no signs of twinning, but had significant dislocation activity which resulted in subgrains throughout the samples. This is shown in Figure 6.

Tantalum was loaded at a strain rate around upper 10^6 s^{-1} . Figures 7 and 8 show the line-outs and σ_E as a function of temperature for tantalum. σ_E measurements were taken by analyzing the material state when the particle velocity is in the trough following the elastic wave.



FIG. 5. TEM of annealed iron which was dynamically loaded at 791 K. Evidence of deformation twinning was found throughout the sample.

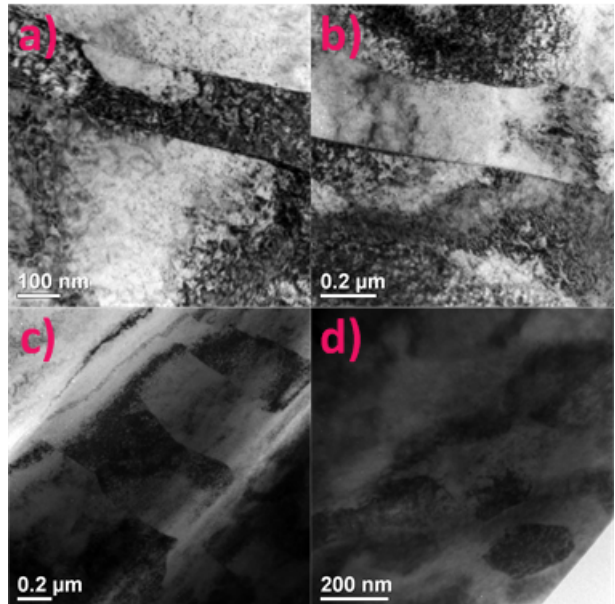


FIG. 6. TEM of recovered as-received iron, a and b corresponding to 160 K and c and d corresponding to 600 K. Both show dislocations throughout and subgrains, with the 600 K having somewhat more subgrain activity.

The strong pullback that results in the trough is likely a outcome of an avalanche of dislocation motion initiated by the high stress in the annealed material. The resulting material state at the trough has somewhat relaxed to the stress state the material tends toward and for this reason is the region of interest in studying the yield behavior of tantalum. The peak of the elastic wave is very time dependent, and given that the resolution of the VISAR is nearly 200 picoseconds whereas the peak is less than

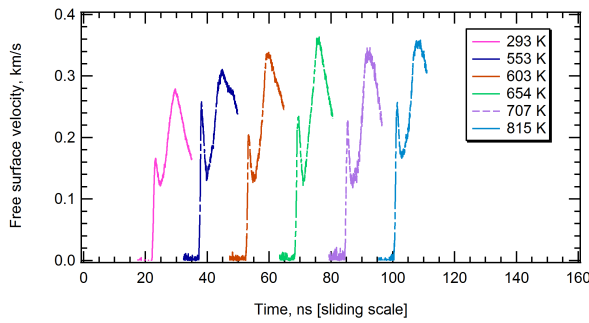
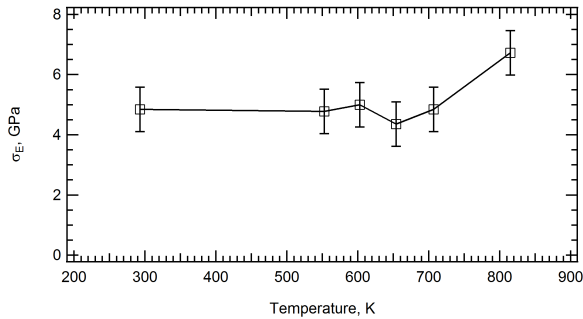


FIG. 7. Tantalum velocimetry as a function of temperature.

FIG. 8. Tantalum σ_E as a function of temperature. Overall, σ_E appears to remain constant with temperature except at 815 K.

100 picoseconds across, it is not wide enough to be accurately resolved. It is worth emphasizing that regarding the peak or the trough as the yield point is a matter of debate, but for this material analysis it was more interesting to study the state at which the material had intends to reach to relieve stress via plastic relaxation. To study the peak accurately would have required a diagnostic with higher temporal resolution without costing the velocity-per-fringe resolution, as this VISAR set-up would have. Based on the analysis techniques outlined, there appears to be a trend of the σ_E remaining constant with with increasing temperature until an anomalous rise at 815 K.

TEM of the shot at 293 K shot showed signs of twinning while TEM of the 815 K shot had no twins. Figures 9 and 10 show micrograph images from each of the recovered samples.

Titanium was loaded at a strain rate around upper 10^6 s^{-1} . It appears that the σ_E is approximately constant over the temperature range. There is not much pullback following the peak elastic stress state, although the material was annealed.

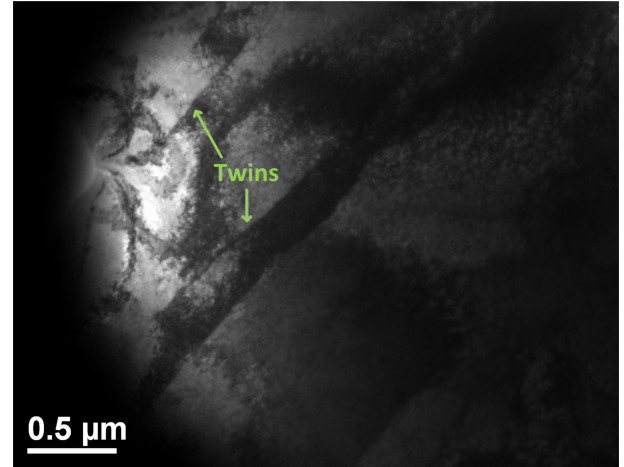


FIG. 9. TEM of recovered tantalum which was shocked at 293 K. Twins were apparent throughout the sample

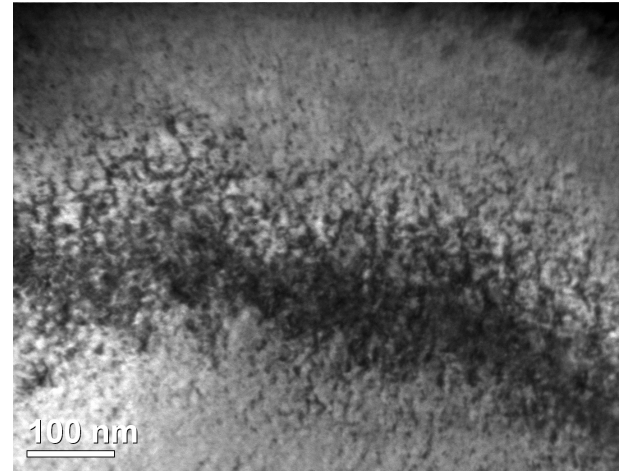


FIG. 10. TEM of recovered tantalum which was shocked at 815 K. No twins were observed, extensive dislocation deformation was evident though.

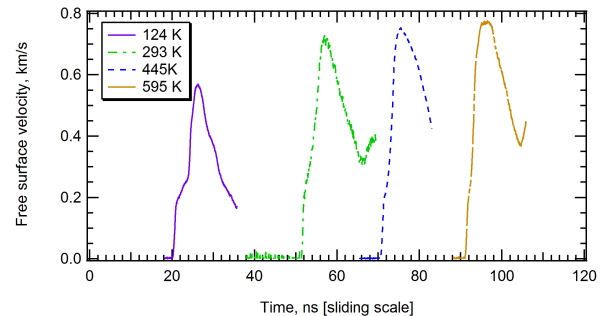


FIG. 11. Titanium line-outs as a function of temperature.

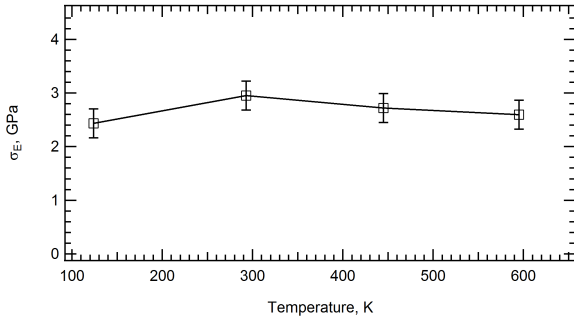


FIG. 12. Titanium σ_E as a function of temperature. There is a general trend of σ_E remaining constant as temperature increases.

IV. DISCUSSION

A. Iron

The σ_E is about 2-3 times higher than low strain rate measurements^{9,36} which is consistent with yield behavior of a material under high strain rate loading. Regarding the differences between the annealed and as-received iron, the as-received is clearly dominated by thermally activated processes whereas the annealed iron seems to exhibit nearly athermal behavior. For the as-received material, the σ_E as well as the peak flow stress at low temperatures is relatively high, which is likely a result of the rate being dominated by dislocation mobility due to the lack of thermal assistance. Additionally, even in relatively pure metals, solutes such as carbon and nitrogen can have noticeable effects on the strength properties^{54,55}. Solute can relieve shear stresses around screw dislocations by orienting themselves into preferential interstitial sites, forming an ordered array around the dislocation^{22,55,56}. This anchors the dislocation, especially at low temperatures. Thermal fluctuations can allow interstitial atoms to rearrange themselves into new preferential interstitial positions as the dislocation traverses through the crystal. At the middle range temperatures, between 275-500 K, thermal activation for overcoming the Peierls stress and depinning dislocations from solute clusters lowers the σ_E . At higher temperatures, above 500 K, it is apparent that the as-received material and the annealed material diverge in σ_E . It can be seen in the TEM images of the recovered as-received iron, shown in Figures 6, that the wormy-shaped dislocations coalesce together to form subgrains. The higher temperature iron showed a higher density of subgrains. This confirms that thermal activation assists in dislocation motion and at higher temperature, the material will be able to relax more easily.

TEM of the annealed iron revealed twins, seen in Figure 5. Twinning in iron has been seen at low temperatures³¹⁻³³ and under shock loading conditions^{19,34,35}. Rohde has noted the change in temperature dependence of a bcc metal between whether it

experiences twinning or slip, with twinning being a nearly athermal process and slip being a strongly thermally activated process¹⁹. Arnold's armco iron data²⁰ also showed a dependence on grain size for twinning vs. slip which Zerilli¹² and Armstrong et al.³⁶ have created constitutive models for that take into account grain size and strain rate. Arnold's data demonstrated that at strain rates 10^3 - 10^6 s⁻¹, the transition from slip to twinning occurred in iron samples of grain sizes of 80 microns. The data presented in this paper shows that for grain structures around 20 microns or less, slip is the dominant mechanism for deformation, whereas for grain sizes on the order of 40 microns or more twinning is the dominant mechanism. That the twinning occurs at slightly smaller grain sizes in the work presented in this paper compared to Arnold's work corresponds to the strain rate dependence of twinning stress shown by Armstrong et al.³⁶. It is worth noting that armco iron is generally around 99.85% purity, which may have some effects compared to the 99.99% purity of the iron studied in this work.

This indicates the need for the right conditions such that either a screw dislocations will either dissociate into partials and the material will twin, or the partials will coalesce and the material will slip. It seems that in the annealed iron, the grain size was large enough that dislocation partials were long enough to overcome line tension, whereas in the as-received iron, the dislocation lengths were likely too small and slip was favored. Using this dynamic data along with Arnold's²⁰, it would be interesting to create a model similar to that implemented by Moulin et al.⁵³ for silicon to determine critical length of dislocation (i.e. grain size) that determines slip to twinning transition. Armstrong et al.⁵⁷ account for twinning deformation in iron and tantalum in their constitutive modelling of high strain rate loading by calculating the activation volume with respect to the burgers vectors of these partials for twinning, reduced from its value corresponding to slip.

B. Tantalum

Tantalum demonstrated a sharp pullback, stronger than the pullback seen in annealed iron. This is thought to be an effect due to the impulsive nucleation of dislocations/twins in an annealed bcc metal which allows rapid relaxation in the material. Other than the strong pullback, the values for σ_E are promisingly consistent with Zaretsky and Kanel's at similar loading conditions on a gas gun²⁵.

At a glance, the overall athermal response would indicate the tantalum had twinned. However, the rise in σ_E at 815 K is outside the error bars and is significant. It is not likely to be dislocation drag since longitudinal and bulk sound speeds were found to be constant across all temperatures; had this been dislocation drag, the sound speeds would have decreased. The drive spot was 1 mm and grain size was approximately 20 microns so it was

not likely an effect of grains. Additionally, the laser drive conditions were well matched between all shots.

TEM of the shot at 293 K shot showed signs of twinning as well as low angle grain boundaries while TEM of the 815 K shot had no twins or grain boundaries. Figures 9 and 10 show micrograph images from each of the recovered samples. It is known that transition between twinning and slip as dominant deformation mechanisms is temperature and strain rate dependent²¹, such that at lower temperatures and higher strain rates, twinning is more prominent. It is possible that through this temperature range at these loading conditions, the materials is transitioning from being twinning dominated to slipping. Like the transition in iron between slip and twinning as rate-controlling mechanisms that happens between grain sizes of merely a couple tens of microns, this transition happens within 100 K. The authors do not know of any dynamic loading experiments that have seen this transition while systematically changing temperature, although this transition in bcc metals is well known to occur quasi-statically and at low strain rates³¹⁻³³. Further experimentation is needed to verify this result and additionally to quantify the discreteness of such a transition with temperature and assess the strain rate dependence of this transition temperature.

Armstrong modelled how dislocation generation at high strain rates raises flow stress in tantalum⁵⁷. It appears the shot at 815 K would be consistent with Armstrong's dislocation generation model. The σ_E in this work is about an order of magnitude higher than the quasistatic and low strain rate strength of tantalum⁶, indicative that under these high strain rate loading conditions the elastic wave has not substantially relaxed, due to nonlinear elastic effects¹⁸. The data is above the critical stress for twinning, approximately between 750-950 MPa⁵⁸. Thus, the twinning to slip transition in tantalum as a function of temperature may be able to account for tantalum's unusual temperature-dependent behavior.

It would be interesting to again use a model similar to Moulin et al.⁵³ to determine critical temperature for partial dissociation and transition from twinning to slip at high pressures. This could be used in physically predictive dislocation dynamics codes which account for loading conditions and initial microstructure to give probability of twinning.

C. Titanium

Titanium varies very little with temperature, likely because of titanium's propensity to twin under shock loading⁷, which empirically has shown to have an approximately athermal trend^{21,59}. It also has considerable strain hardening after the σ_E , indicating there is an appreciable initial dislocation density that impedes plastic flow. The values of σ_E are significantly higher than the values Chichili et al.⁷ at strain rates up to 10^5 s⁻¹. The magnitude of this increase, approximately threefold, is

	Temperature, K	Elastic wave speed, m/s	HEL wave speed, m/s
Tantalum	293	4516	4288
	553	4490	4318
	603	4465	4288
	654	4461	4242
	707	4461	4262
	815	4487	4265

TABLE I. Table of sound speeds deduced from arrival of elastic wave and onset of plasticity as a function of temperature in tantalum. Sound speed uncertainty was ± 70 m/s.

substantial but not anomalous, and is comparable strain rate-dependent behavior of iron⁹.

D. Comparison to fcc metals

In all cases, longitudinal sound speed and bulk sound speed do not lower with temperature, and there is no marked increase of σ_E with temperature, which indicates that lattice drag arising from anharmonic phonon interactions¹⁸ does not have a prominent effect. This particularly is important to note in tantalum, since the unexpected rise in σ_E at 815 K could easily be presumed to be an effect of dislocation drag. One would not necessarily expect these metals to have the same strong indication of nonlinear elastic effects on the temperature dependence of σ_E that has been seen in other metals like aluminum, copper, and silver^{16,60,61} because these metals do not present strong indications of phonon anharmonicity, as suggested by their comparatively lower Gruneisen parameters¹⁸.

V. CONCLUSION

The dynamic strength properties of annealed and as-received iron as well as tantalum and titanium were studied using a high powered laser system in an effort to further understand the effect of temperature and microstructure on transition metals. Experimental results showed the role dislocation density and grain size plays can have a large effect on the temperature dependence of the onset of plastic flow, as seen in the annealed iron and the as-received iron. It seems that the as-received iron was dislocation mobility limited and would yield more readily at higher temperatures due thermal assistance in overcoming Peierls' barriers, resulting in dislocations coalescing into subgrains, while the annealed iron had undergone significant deformation twinning. Tantalum also twinned and exhibited a temperature dependence similar to the annealed iron, however the tantalum had a stronger, sharper pullback. Tantalum experienced a transition to slip-mediated plasticity at 815 K. Titanium exhibited an athermal response, typical of twinning be-

havior in this material. This all demonstrates the complexity of predicting material behavior, accounting for thermal activation, twinning vs. slip, dislocation generation vs. mobility, and dislocation drag.

VI. ACKNOWLEDGEMENTS

This work performed under the auspices of the U.S. Department of Energy by Lawrence Livermore National Laboratory under Contract DE-AC52-07NA27344 (LLNL-JRNL-XXXXXX). Chen and Bernier gratefully acknowledge funding under the Laboratory Directed Research and Development program (LDRD 13-ERD-078). The Institute of Shock Physics acknowledges the support of AWE and Imperial College London. The authors would like to thank the Trident Laser Facility staff at Los Alamos National Laboratory for their generous support during experiments which made this work possible. The authors would like to thank Ecaterina Ware, Mahmoud Ardakani, and Ayan Bhowmik of Imperial College London for their help with the microscopy performed in this work.

VII. REFERENCES

- ¹R. Clifton and X. Markenscoff, "Elastic precursor decay and radiation from nonuniformly moving dislocations," *Journal of the Mechanics and Physics of Solids* **29**, 227–251 (1981).
- ²R. J. Clifton, "Dynamic Plasticity," *Journal of Applied Mechanics* **36**, 382 (1983).
- ³B. n. Gurrutxaga-Lerma, D. S. Balint, D. Dini, D. E. Eakins, and A. P. Sutton, "Attenuation of the Dynamic Yield Point of Shocked Aluminum Using Elastodynamic Simulations of Dislocation Dynamics," *Physical Review Letters* **114**, 1–5 (2015).
- ⁴P. Follansbee and J. Weertman, "On the Question of Flow Stress At High Strain Rates Controlled By Viscous Flow," *Mechanics of Materials* , 345–350 (1982).
- ⁵P. S. Follansbee and U. F. Kocks, "A constitutive description of the deformation of copper based on the use of the mechanical threshold stress as an internal state variable," *Acta Metallurgica* **36**, 81–93 (1988).
- ⁶K. Hoge and A. Mukherjee, "The temperature and strain rate dependence of the flow stress of tantalum," *Journal of Materials Science* **12**, 1666–1672 (1977).
- ⁷D. Chichili, K. Ramesh, and K. Hemker, "The high-strain-rate response of alpha-titanium: experiments, deformation mechanisms and modeling," *Acta Materialia* **46**, 1025–1043 (1998).
- ⁸U. Andrade, M. Meyers, K. Vecchio, and A. Chokshi, "Dynamic recrystallization in high-strain, high-strain-rate plastic deformation of copper," *Acta Metallurgica et Materialia* **42**, 3183–3195 (1994).
- ⁹R. F. Smith, J. H. Eggert, R. E. Rudd, D. C. Swift, C. A. Bolme, and G. W. Collins, "High strain-rate plastic flow in Al and Fe," *Journal of Applied Physics* **110** (2011), 10.1063/1.3670001.
- ¹⁰J. Wang, "Prediction of Peierls stresses for different crystals," *Materials Science and Engineering: A* **206**, 259–269 (1996).
- ¹¹F. J. Zerilli and R. W. Armstrong, "Dislocation-mechanics-based constitutive relations for material dynamics calculations," *Journal of Applied Physics* **61**, 1816 (1987).
- ¹²F. J. Zerilli, "Dislocation Mechanics Based Constitutive Equations," *Metallurgical and Materials Transactions A* **35**, 2547–2555 (2004).
- ¹³R. W. Armstrong and S. M. Walley, "High strain rate properties of metals and alloys," *International Materials Reviews* **53**, 105–128 (2008).
- ¹⁴G. I. Kanel, S. V. Razorenov, A. Bogatch, A. V. Utkin, V. E. Fortov, and D. E. Grady, "Spall fracture properties of aluminum and magnesium at high temperatures," *Journal of Applied Physics* **79**, 8310 (1996).
- ¹⁵A. V. Utkin, G. I. Kanel, S. V. Razorenov, A. A. Bogach, and D. E. Grady, "Elastic moduli and dynamic yield strength of metals near the melting temperature," *AIP Conference Proceedings* **443**, 443–446 (1998).
- ¹⁶S. V. Razorenov, G. L. Kanel, K. Bamming, and H. J. Bluhm, "Hugoniot elastic limit and spall strength of aluminum and copper single crystals over a wide range of strain rates and temperatures," *Shock Compression of Condensed Matter* , 2–5 (2002).
- ¹⁷G. I. Kanel, "Rate and temperature effects on the flow stress and tensile strength of metals," in *AIP Conference Proceedings*, Vol. 939 (2012) pp. 939–944.
- ¹⁸L. E. Chen, D. C. Swift, R. A. Austin, J. N. Florando, J. Hawrelak, A. Lazicki, M. D. Saculla, D. E. Eakins, J. V. Bernier, and M. Kumar, "Temperature and strain rate dependence of plastic flow due to nonlinear elastic effects in fcc metals aluminum and invar," Submitted (2015).
- ¹⁹R. Rohde, "Dynamic yield behavior of shock-loaded iron from 76 to 573 K," *Acta Metallurgica* (1969).
- ²⁰W. Arnold, "Dynamisches Werkstoffverhalten von Armco-Eisen bei Stoss-wellenbelastung," (1992).
- ²¹M. A. Meyers, O. Vohringer, and V. A. Lubarda, "The onset of twinning in metals: a constitutive description," *49*, 4025–4039 (2001).
- ²²J. H. Bechtold, "Tensile Properties of Annealed Tantalum at Low Temperatures," *Acta Metallurgica* **3**, 249–254 (1955).
- ²³S. R. Chen and G. T. G. Ill, "Constitutive Behavior of Tantalum and Tantalum-Tungsten Alloys," *27* (1996).
- ²⁴S. Nemat-Nasser, T. Okinaka, and L. Ni, "A physically-based constitutive model for bcc crystals with application to polycrystalline tantalum," *46*, 1009–1038 (1998).
- ²⁵E. B. Zaretsky and G. I. Kanel, "Tantalum and vanadium response to shock-wave loading at normal and elevated temperatures. Non-monotonic decay of the elastic wave in vanadium," *Journal of Applied Physics* **115**, 243502 (2014).
- ²⁶T. S. Duffy and T. J. Ahrens, "Dynamic response of molybdenum shock compressed at 1400C," *Journal of Applied Physics* **76**, 835 (1994).
- ²⁷T. de Rességuier, E. Lescoute, and D. Loison, "Influence of elevated temperature on the wave propagation and spallation in laser shock-loaded iron," *Physical Review B* **86**, 214102 (2012).
- ²⁸E. M. Bringa, A. Caro, Y. Wang, M. Victoria, J. M. McNaney, B. a. Remington, R. F. Smith, B. R. Torralva, and H. Van Swygenhoven, "Ultrahigh strength in nanocrystalline materials under shock loading," *Science* **309**, 1838–41 (2005).
- ²⁹M. Meyers, F. Gregori, B. Kad, M. Schneider, D. Kalantar, B. Remington, G. Ravichandran, T. Boehler, and J. Wark, "Laser-induced shock compression of monocrystalline copper: characterization and analysis," *Acta Materialia* **51**, 1211–1228 (2003).
- ³⁰M. a. Meyers, M. S. Schneider, H. Jarmakani, B. Kad, B. a. Remington, D. H. Kalantar, J. McNaney, B. Cao, and J. Wark, "Deformation substructures and their transitions in laser shock-compressed copper-aluminum alloys," *Metallurgical and Materials Transactions A: Physical Metallurgy and Materials Science* **39**, 304–321 (2008).
- ³¹H. W. Paxton, "Experimental verification of the twin system in alpha-iron," *Acta Metallurgica* , 1–5 (1953).
- ³²W. D. Biggs and P. L. Pratt, "The deformation and fracture of alpha-iron at low temperatures," *Acta Materialia* **6** (1958).

³³S. Ikeda and T. Takeuchi, "Stress and delay time for the appearance of twinning deformation in iron single crystals," *Journal of the Physical Society of Japan* (1965).

³⁴J. N. Johnson and R. W. Rohde, "Dynamic deformation twinning in shock-loaded iron," *Journal of Applied Physics* **42**, 4171–4182 (1971).

³⁵J. W. Taylor and M. H. Rice, "Elastic-Plastic Properties of Iron," *Journal of Applied Physics* **34**, 364–371 (1963).

³⁶R. W. Armstrong, "Strength and strain rate sensitivity of nanopolycrystals," in *Mechanical Properties of Nanocrystalline Materials*, edited by J. C. M. Li (Pan Stanford Publishing, C/o World Scientific Publishing Co., Inc.; Hackensack, NJ, 2009) Chap. 3, pp. 1–34.

³⁷A. H. Cottrell and B. A. Bilby, "A mechanism for the growth of deformation twins in crystals," *Philosophical Magazine* **42**, 573–581 (1951).

³⁸J. A. Venables, "Deformation twinning in face-centred cubic metals," *Philosophical Magazine* **6**, 379–396 (1961).

³⁹J. B. Cohen and J. Weertman, "A dislocation model for twinning in fcc metals," *Acta Metallurgica* (1963).

⁴⁰J. A. Venables, "The nucleation and propagation of deformation twins," *J. Phys. Chem. Solids* **25**, 693–700 (1964).

⁴¹A. W. Sleeswyk, "Perfect dislocation pole models for twinning in the f.c.c. and b.c.c lattices," *Philosophical Magazine* **29**, 407–421 (1974).

⁴²J. P. Hirth and J. Lothe, *Theory of Dislocations* (John Wiley & Sons, Inc., 1992).

⁴³J. Christian and S. Mahajan, "Deformation twinning," *Progress in Materials Science* **39**, 1–157 (1995).

⁴⁴J. Sanchez, L. Murr, and K. Staudhammer, "Effect of grain size and pressure on twinning and microbanding in oblique shock loading of copper rods," *Acta Materialia* **45**, 3223–3235 (1997).

⁴⁵K. P. D. Lagerlof, J. Castaing, P. Pirouz, and A. H. Heuer, "Nucleation and growth of deformation twins: a perspective based on the double-cross-slip mechanism of deformation twinning," *Philosophical Magazine A* **82**, 2841–2854 (2002).

⁴⁶S. Mahajan and G. Y. Chin, "Formation of deformation twins in f.c.c. crystals," **21** (1973).

⁴⁷S. Mahajan, "Critique of mechanisms of formation of deformation, annealing and growth twins: Face-centered cubic metals and alloys," *Scripta Materialia* **68**, 95–99 (2013).

⁴⁸O. Bouaziz, S. Allain, C. Scott, P. Cugy, and D. Barbier, "High manganese austenitic twinning induced plasticity steels-A review of the microstructure properties relationships..pdf," *Current Opinion in Solid State Materials Science* , 141–168 (2011).

⁴⁹S. Mahajan, "Interrelationship between slip and twinning in b.c.c. crystals," *Acta Metallurgica* (1975).

⁵⁰K. Lagerlof, "On deformation twinning in b.c.c. metals," *Acta Metallurgica et Materialia* **41**, 2143–2151 (1993).

⁵¹H. Fujita and T. Mori, "A formation mechanism of mechanical twins in F.C.C. Metals," *Scripta Metallurgica* **9**, 631–636 (1975).

⁵²P. Pirouz, "Deformation mode in silicon, slip or twinning?" *Scripta Metallurgica* **21**, 1463–1468 (1987).

⁵³A. Moulin, M. Condat, and L. P. Kubin, "Perfect and partial Frank-Read sources in silicon: a simulation," *Philosophical Magazine A* **79**, 1995–2011 (1999).

⁵⁴J. Snoek, "Effect of small quantities of carbon and nitrogen on the elastic and plastic properties of iron," *Physica* **8**, 711–733 (1941).

⁵⁵A. Cottrell and B. Bilby, "Dislocation Theory of Yielding and Strain Ageing of Iron," *Proceedings of Physical Society* , 49–62 (1949).

⁵⁶F. Nabarro, "Mechanical Effects of Carbon in Iron," in *Physical Society Bristol Conference Proc.* (1948) pp. 38–45.

⁵⁷R. Armstrong, W. Arnold, and F. Zerilli, "Dislocation Mechanics of Shock-Induced Plasticity," *Metallurgical and Materials Transactions A* **38**, 2605–2610 (2007).

⁵⁸L. E. Murr, M. A. Meyers, C.-S. Niou, Y. J. Chen, S. Pappu, and C. Kennedy, "Shock-induced deformation twinning in tantalum," *Acta Metallurgica* **45**, 157–175 (1997).

⁵⁹W. Holt, W. Mock, F. Zerilli, and J. Clark, "Experimental and computational study of the impact deformation of titanium Taylor cylinder specimens," *Mechanics of Materials* **17**, 195–201 (1994).

⁶⁰E. B. Zaretsky and G. I. Kanel, "Effect of temperature, strain, and strain rate on the flow stress of aluminum under shock-wave compression," *Journal of Applied Physics* **112**, 073504 (2012).

⁶¹E. B. Zaretsky and G. I. Kanel, "Plastic flow in shock-loaded silver at strain rates from 104 s⁻¹ to 107 s⁻¹ and temperatures from 296 K to 1233 K," *Journal of Applied Physics* **110** (2011), 10.1063/1.3642989.

⁶²H. K. Mao, W. A. Bassett, and T. Takahashi, "Effect of pressure on crystal structure and lattice parameters of iron up to 300 kbar," *Journal of Applied Physics* **38**, 272–276 (1967).

⁶³D. Errandonea, Y. Meng, M. Somayazulu, and D. Häusermann, "Pressure-induced alpha - omega transition in titanium metal: A systematic study of the effects of uniaxial stress," *Physica B: Condensed Matter* **355**, 116–125 (2005), arXiv:0401549 [cond-mat].

⁶⁴A. Dewaele and P. Loubeyre, "Mechanical properties of tantalum under high pressure," *Physical Review B - Condensed Matter and Materials Physics* **72**, 1–9 (2005).